

Surface Modification and Deuterium Retention in Reduced Activation Ferritic Martensitic Steels Exposed to Low-Energy, High Flux D Plasma and D₂ Gas

V.Kh. Alimov^{a,b}, Y. Hatano^b, K. Sugiyama^a, M. Balden^a, T. Höschen^a, M. Oyaidzu^c, J. Roth^a,
J. Dorner^a, M. Fußeder^a, T. Yamanishi^c

^a*Max-Planck-Institut für Plasmaphysik, EURATOM Association, 85748 Garching, Germany,*

^b*Hydrogen Isotope Research Center, University of Toyama, Toyama, 930-8555 Japan,*

^c*Tritium Technology Group, Japan Atomic Energy Agency, Rokkasho, 039-3212 Japan*

E-mail: vkahome@mail.ru (V.Kh. Alimov)

Abstract

Samples prepared from steels F82H and EUROFER97 were irradiated with 20 MeV W ions at 300 K to 0.75 displacements per atom. Damaged and undamaged samples were exposed at elevated temperatures to deuterium plasma at ion energies of 60 and 200 eV to a fluence of $\approx 10^{26}$ D/m² and to D₂ gas at a pressure of 100 kPa. The surface modification after plasma exposure was examined by scanning electron microscopy and Rutherford backscattering spectroscopy. Deuterium depth profiles were determined by the D(³He, p)⁴He nuclear reaction. In damaged steels loaded with deuterium, deuterium decorates the damage profile, and the D concentrations decreasing with increasing temperature. After exposure of the F82H steel to the D plasma, W-enriched near-surface layers are formed. The effective concentration of W in the near-surface steel layer depends on plasma exposure conditions.

PACS numbers: 52.40.Hf, 61.80.Jh

1. Introduction

Reduced Activation Ferritic Martensitic (RAFM) steels are the primary choice material for first wall and breeding blanket structural application in future fusion power plants [1, 2, 3]. These steels have been developed in order to simplify special waste storage of highly radioactive structures of fusion reactor after service. With this objective some alloying elements such as Mo, Nb and Ni present in the commercial martensitic steels have been replaced by other elements which exhibit faster decay of induced radioactivity such as Ta, W and V [4].

In most scenarios the RAFM structural steel components are assumed to be protected from erosion by several mm thick tungsten (W) armors. Nevertheless, disadvantages of bulk W proposed as first-wall plasma facing material in future DEMO reactor [5] are its heavy weight and poor workability. Furthermore, pure W is brittle, and its material properties degrade due to neutron irradiation. On the other hand, the use of bare RAFM steel as first-wall material in a fusion reactor, at least in selected areas of the main chamber, has been proposed in the past [6]. From inspection of the sputtering yields and comparison to those of tungsten (where sputtering by hydrogen isotope particles is negligible), steel should be regarded as viable plasma facing material option. It can be expected that, due to the difference in sputtering yields between low-Z and high-Z materials with hydrogen isotope particles [7], the near-surface layer of the steel will be enriched with W and the erosion yield, in consequence, will be reduced.

As probable plasma-facing material, RAFM steel will be subjected to intensive fluxes of energetic deuterium (D) and tritium (T) as well as 14 MeV neutrons (n) from the D–T fusion reaction. One possibility to investigate the influence of n-produced defects on the hydrogen isotope inventory is to simulate displacement damage using irradiation with energetic heavy ions [8] before exposing to energetic D ions.

The objective of this work is to study (i) modification of the surface composition of RAFM steels under exposure to low-energy, high-flux D plasma at various temperatures and (ii) deuterium retention at the ion-induced displacement damage in RAFM steels after exposure to the D plasma and D₂ gas at elevated temperatures.

2. Experimental

Two RAFM steels were used in this work: F82H (Japan) [4] and EUROFER97 (EU) [3]. It is appropriate to mention that main alloying elements of these steels, along with low Z

elements (C, Fe, Cr, Mn, V, N, P, S, B, O), are high Z elements such as W (≈ 1.9 wt.% in F82H and 1.0-1.2 wt.% in EUROFER97) and Ta (≈ 0.02 wt.% in F82H and 0.10-0.14 wt.% in EUROFER97) [9]. Rectangular-shape RAFM steel samples, 10×10 mm² (F82H) and 12×15 mm² (EUROFER97) in size and 1 mm in thickness, were cut from slabs of each material followed by mechanical polishing to a high finish and cleaning in an ultrasonic bath.

The square-shaped RAFM samples were irradiated with 20 MeV W ions at 300 K to fluence of 8×10^{17} W/m². As a result, the near-surface layer of the samples was damaged to 0.75 displacements per atom (dpa) at the damage peak situated at a depth of 1.9 μ m. The damage profile in Fe target was calculated using the program SRIM 2008.03 [10], “full cascade option”, with the displacement energy of $E_d = 40$ eV. In what follows the W-ion-irradiated steel samples will be designated as “damaged” samples.

In the first set of experiments, the undamaged and damaged F82H samples were exposed to low-energy, high-flux deuterium plasma in the linear plasma generator [11] at temperatures in the range from 325 to 770 K, and the damaged samples were exposed on the damaged side. The steel sample was fixed in the target holder with the help of a Mo ring. The D plasma was composed of species of D_2^+ (over 80%) and D^+ (less than 20%) [11]. A bias voltages of -64 V and -204 V were applied to the steel samples, resulting in incident energies of 60 and 200 eV, correspondingly, for deuterium ions, taking into account the plasma potential of about -4 V as measured by a Langmuir probe. Below we will indicate the ion energy having in mind that this energy is for D^+ and D_2^+ . The incident deuterium ion flux and fluence were fixed at $\approx 10^{22}$ D/m²s and $\approx 10^{26}$ D/m², respectively. The exposure temperature was set by the thermal contact between the sample and the water-cooled holder. The temperature was monitored using a type K thermocouple tightly pressed the rear of the sample.

In the second set of experiments, the damaged F82H and EUROFER97 samples were exposed to D₂ gas at a pressure of 100 kPa and temperatures of 373 K for 10 h, and 473 and 573 K for 5 h. The sample was placed inside the quartz tube connected to the high-vacuum pumping system and heated in a vacuum with the use of an external ohmic heater. The temperature was monitored using a type K thermocouple contacted directly to the sample inside the tube. As the sample temperature reached the required value, a valve between the tube and the pumping system was closed and the tube was filled with D₂ gas. The background pressure inside the tube was measured with an ionization gauge, whereas the D₂ gas pressure was controlled with a Baratron capacitance manometer. After reaching required exposure

duration, D₂ gas evacuation and sample cooling started simultaneously. D₂ gas was evacuated in several seconds, while the sample was cooled down in several minutes.

After exposure to the D plasma, the surface topography and three-dimensional subsurface morphology of the steel samples were examined by a field emission SEM combined with a focused ion beam (HELIOS NanoLab 600, FEI) [12]. The concentration of high-Z materials in the steel near-surface layer was determined by means of Rutherford backscattering spectroscopy (RBS) at ⁴He ion energy of 3 MeV and an incident angle of 75° to the surface normal and at a scatter angle of 165°. The RBS spectra were evaluated with the program SIMNRA [13]. In addition, the chemical composition in the outermost atomic layers on the steel surface was determined by X-ray photoelectron spectroscopy (XPS).

The deuterium depth profiles in the steel samples were determined by nuclear reaction analysis (NRA). The D(³He, p)⁴He reaction was utilized, and both the α particles and protons were analyzed. The α-spectrum was transformed into a D depth profile at depths up to ≈0.5 μm using the program SIMNRA [13]. To determine the D concentration at larger depths, the energy of the analyzing beam of ³He ions was varied from 0.69 to 4.0 MeV. The proton yields measured at different ³He ion energies allow D depth profiles to be measured to depths of up to 7 μm [14].

3. Results and discussion

3.1. Surface composition of F82H steel after D plasma exposure

Evaluation of RBS and XPS spectra allows the conclusion that D plasma exposure of the F82H steel with ions fluence of 10²⁶ D/m² leads to an enrichment of the near-surface layer with W due to preferential sputtering of Fe. The Ta content in the near-surface layer is still below the detection limit of XPS. Due to sputtering of the Mo ring holding the steel sample, the near-surface layer contains also deposited molybdenum. After D plasma exposure with the ion energy of 60 eV at $T_{\text{exp}} = 365$ K, the effective concentration of W, as evaluated from RBS spectra by assuming smooth surfaces and homogeneous distributions, reaches a value of ≈4 at.%, whereas the effective concentration of the deposited Mo is ≈1 at.%. However, as the ion energy rises to 200 eV, the W effective concentration in the near-surface layer is increased and reaches ≈20 at.% at $T_{\text{exp}} = 460$ K and ≈30 at.% at $T_{\text{exp}} = 770$ K. The Mo effective concentration for the both exposure temperatures is ≈10 at.%.

SEM images of the F82H steel exposed to the D plasma demonstrate that the surface morphology depends strongly on the ion energy and exposure temperature (Fig. 2). After 60

eV D plasma exposure at $T_{\text{exp}} = 365$ K, the roughness of the surface is around 50 nm (Fig. 2a). However, exposures with 200 eV D plasma at elevated temperatures lead to formation of nano-structured near-surface layers. At $T_{\text{exp}} = 460$ K column-like structure of 300 nm in thickness is observed (Fig. 2b), whereas at $T_{\text{exp}} = 770$ K coral-like structure of up to 2 μm in thickness is formed (Fig. 2c). We have not enough data to discuss mechanisms of formation of these structures in this paper. However, observation of these structures allows the conclusions that (i) the broadening in the RBS depth profiles of the high-Z element could be due to the surface roughness [13], and (ii) the effective concentrations of W and Mo given in Fig. 1 are lower limit for the enrichment.

Note that for D plasma exposures at the same conditions, the surface morphology of the damaged F82H samples is comparable to the undamaged ones. Thus, the irradiation with 20 MeV W ions has no noticeable influence on the steel surface morphology after D plasma exposure.

3.2. Deuterium retention in RAFM steels

In the undamaged F82H steel exposed to the 60 eV D plasma at 365 K, the deuterium depth profile is characterized by a sharp near-surface concentration maximum of $\approx 4 \times 10^{-2}$ at.%, and, at depths above 1 μm , by a concentration of $\approx 6 \times 10^{-3}$ at.%, then slowly decreasing into the bulk (Fig. 3a). As the ion energy and exposure temperature increases to 200 eV and 460 K, correspondingly, the D concentration in the near-surface layers increases to ≈ 0.2 at.%, whereas the concentration at depths of 2-7 μm amounts to $\approx 6 \times 10^{-3}$ at.%. An increase of the D concentration in the near-surface with increasing of exposure temperature can be possibly explained by an increase of the D ion energy and/or an enrichment of the near-surface layer with W. Further increase of the exposure temperature at the same ion energy of 200 eV leads to a decrease of the D concentration at depths of up to 2-3 μm and to an increase at greater depths (Fig. 3a). The concentration minimum at depths of 1-4 μm observed after D plasma exposure at 770 K is thought to be connected with the appearance of the coral-like near-surface structure and accompanying porosity development.

Generation of W-ion-induced displacement damage and subsequent exposure to the D plasma significantly increases the D concentration at depths up to about 3 μm (i.e., in the damage zone) (Fig. 3b). The D concentration decreases with increasing temperature. Strong temperature dependence of the D concentration in the damage zone is also observed in damaged F82H and EUROFER97 steels exposed to D_2 gas at a pressure of 100 kPa and

various temperatures (Fig. 4). Both materials demonstrate the same D retention behavior. After D₂ exposure at $T_{\text{exp}} = 373$ K for 10 h, deuterium is retained mainly at depths of less than 1 μm . Obviously, at these exposure condition the flux of D atoms diffusing into the bulk is low, and D atoms decorate only the near-surface part of the W-ion-induced defects. However, after exposure to D₂ gas at 473 and 573 K for 5 h, deuterium is retained over the whole damage zone to a concentration depending on the exposure temperature (Fig. 4). In doing so, the D concentration reaches saturation, as shown from comparison between D depth profiles after exposures at 473 K for 5 and 50 h. Note that for D₂ exposure at 473 K, the D concentration beyond the damage zone increases by a factor of about three (from $\approx 3 \times 10^{-4}$ to $\approx 10^{-3}$ at.%) as the exposure duration is extended from 5 to 50 h (Fig. 4b).

In the damaged RAFM steels exposed either to the D plasma or D₂ gas, the D concentration at the depth of the damage peak, $^{\text{damage}}C_{\text{D}}$, decreases as the exposure temperature increases (Fig. 5). Interestingly, the concentration $^{\text{damage}}C_{\text{D}}$ observed after D plasma exposure at $T_{\text{exp}} = 425$ K is significantly lower than that after D₂ gas exposure at $T_{\text{exp}} = 473$ K. It is appropriate to mention here that similar effect was observed for W exposed at about 700 K to the low-energy, high-flux D plasma and D₂ gas at 100 kPa [8].

Analyzing data on the D concentration in the damage zone observed after exposures of the damaged steels to D plasma and D₂ gas, it is necessary to keep in mind that at the same concentration of the ion-induced defects, the saturation value of the D concentration in the damage zone depends both on the exposure temperature and the concentration of D atoms in solute state, $^{\text{sol}}C_{\text{D}}$, maintained under the plasma or gas exposures [8, 15]. The concentration $^{\text{sol}}C_{\text{D}}$ in the RAFM steels can be estimated for D₂ gas exposure [16, 17] and is unknown for the D plasma exposure. One can assume that under D plasma exposure at 425 K the concentration $^{\text{sol}}C_{\text{D}}$ is lower than that under D₂ gas exposure at 473 K.

4. Summary

After exposure of F82H steel to low-energy (60 and 200 eV), high-flux D plasma, W-enriched near-surface layers are formed due to preferential sputtering of Fe. The effective concentration of W in the steel near-surface layer varies from ≈ 4 to ≈ 30 at.%, depending on plasma exposure conditions. After D plasma exposure at ion energy of 60 eV and exposure temperature of 365 K, the steel surface is relatively smooth and the roughness of the surface is around 50 nm. However, an increase of the ion energy to 200 eV leads to formation of nano-

structured near-surface layers, namely, to 300 nm thick column-like structure at $T_{\text{exp}} = 460$ K and around 2 μm thick coral-like structure at $T_{\text{exp}} = 770$ K.

In F82H and EUROFER97 steels irradiated with 20 MeV W ions at 300 K to the damage level of 0.75 dpa at the damage peak and then exposed to D plasma and D₂ gas, deuterium decorates the damage profile. The saturation value of the D concentration in the damage zone decreases with increasing exposure temperature and varies from $\approx 10^{-1}$ at.% at $T_{\text{exp}} = 325$ K to $\approx 5 \times 10^{-3}$ at.% at $T_{\text{exp}} = 425$ K for D plasma exposure, and from $\approx 3 \times 10^{-2}$ at.% at $T_{\text{exp}} = 473$ K to $\approx 10^{-3}$ at.% at $T_{\text{exp}} = 573$ K for D₂ gas exposure. One can assume that the saturation D concentration in the damage zone of the RAFM steels depends both on the exposure temperature and the concentration of D atoms in solute state.

Acknowledgements

The authors would like to thank Dr. H. Tanigawa (JAEA) for providing F82H samples. This work was partly supported by Broader Approach Activities in Rokkasho, Japan.

Figure captions

Figure 1. Effective concentration of W and Mo in the near-surface layers of undamaged F82H steel exposed to low-energy, high-flux D plasma at ion energies of 60 and 200 eV and temperatures of 365, 460, and 770 K to an ion fluence of $\approx 10^{26}$ D/m², as determined by RBS technique. Deuterium ion energies and exposure temperatures are indicated in the legend. The arrow indicates a depth of about 30 nm.

Figure 2. SEM images of undamaged F82H steel exposed to low-energy, high-flux D plasma at ion energies of 60 eV (a) and 200 eV (b, c) and temperatures of 365 K (a), 460 K (b), and 770 K (c) to an ion fluence of $\approx 10^{26}$ D/m². Only the surface on panel (b) was tilted by 52° to the electron beam.

Figure 3. Depth profiles of deuterium retained in undamaged (a) and damaged (b) F82H steel after exposure to low-energy, high-flux D plasma at ion energy of 60 and 200 eV and various temperatures to an ion fluence of $\approx 10^{26}$ D/m². Deuterium ion energies and exposure temperatures are indicated in the legend. Damage depth profile, as calculated by SRIM 2008.03 [10], is also shown.

Figure 4. Depth profiles of deuterium retained in damaged F82H (a) and EUROFER97 (b) steels after exposure to D₂ gas at a pressure of 100 kPa. Exposure temperatures and exposure durations are indicated in the legends. In both panels, damage depth profile, as calculated by SRIM 2008.03 [10], is also shown.

Figure 5. Concentration of deuterium retained at a depth of the damage peak in damaged F82H and EUROFER97 steels exposed to low-energy, high-flux D plasma and to D₂ gas, as a function of exposure temperature. Conditions of deuterium loading are indicated in the legend.

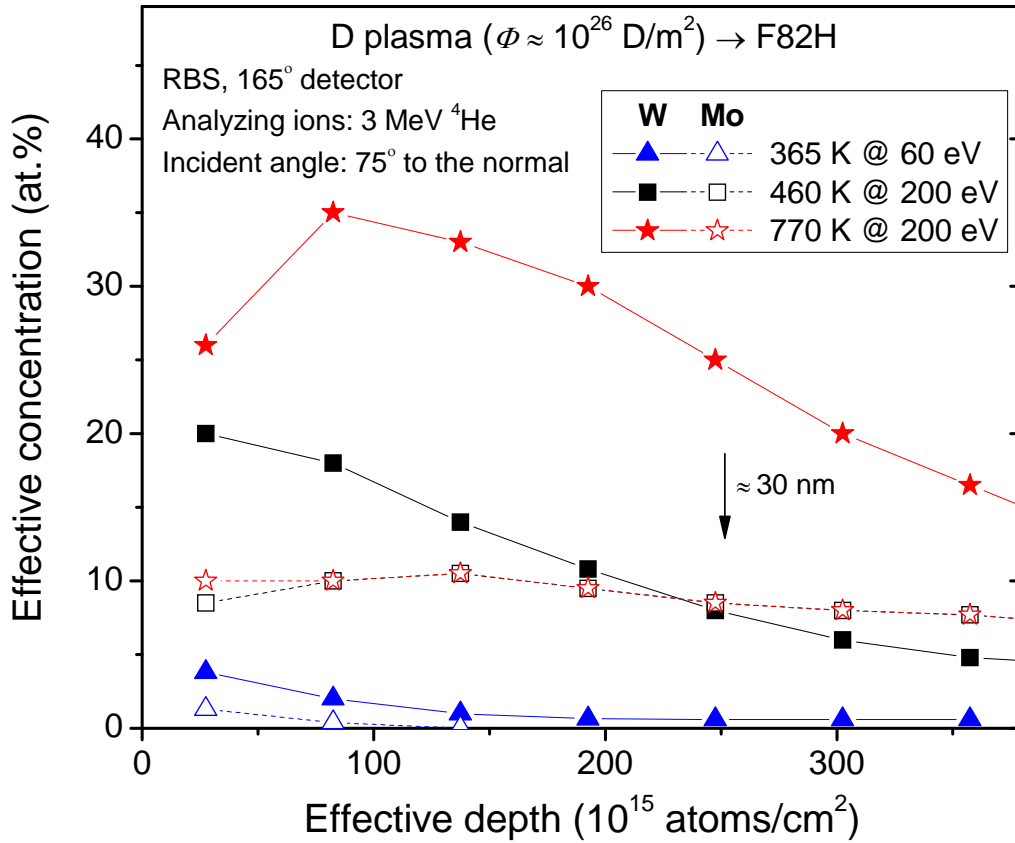


Figure 1. Effective concentration of W and Mo in the near-surface layers of undamaged F82H steel exposed to low-energy, high-flux D plasma at ion energies of 60 and 200 eV and temperatures of 365, 460, and 770 K to an ion fluence of $\approx 10^{26}$ D/m², as determined by RBS technique. Deuterium ion energies and exposure temperatures are indicated in the legend. The arrow indicates a depth of about 30 nm.

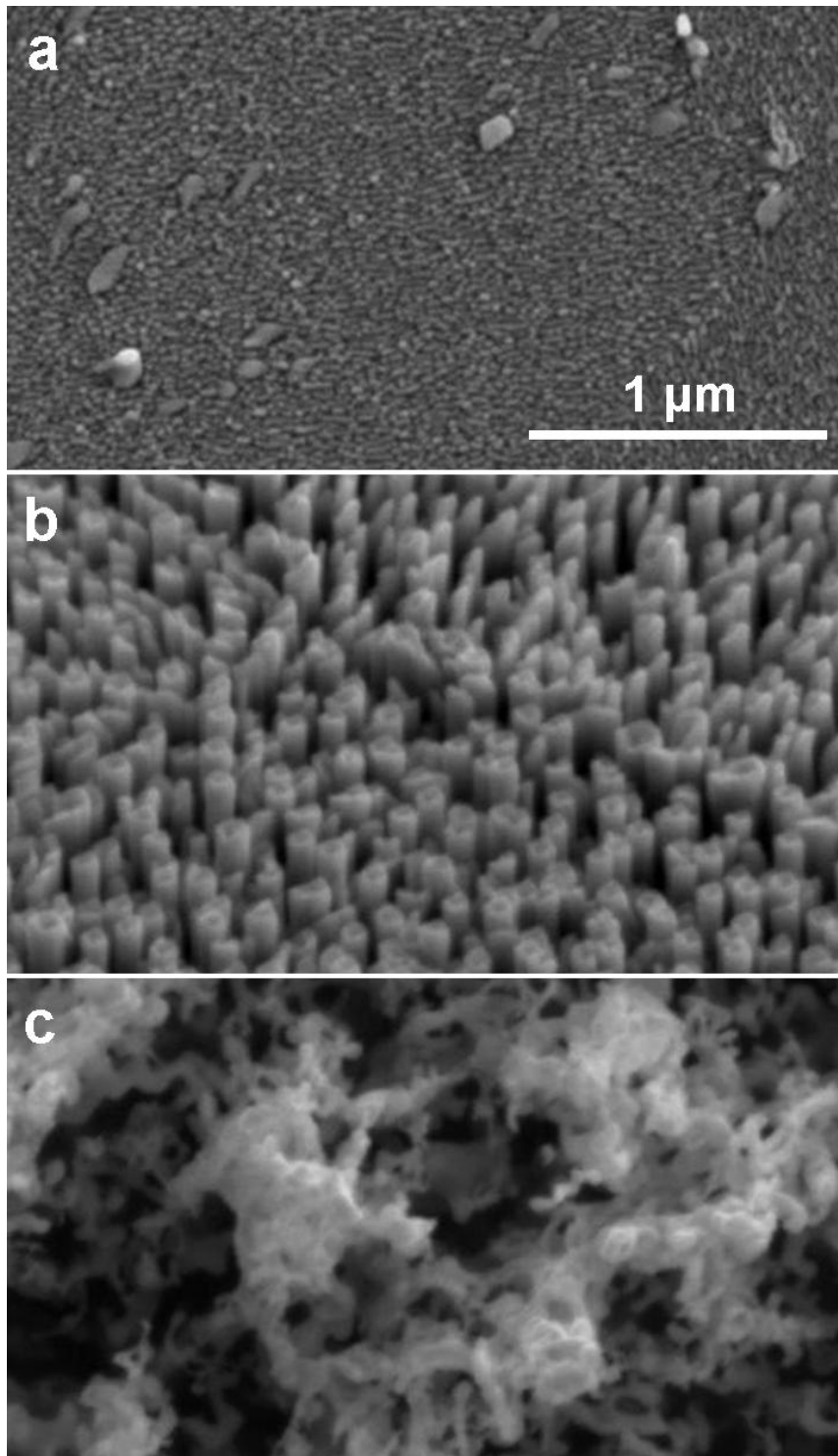


Figure 2. SEM images of undamaged F82H steel exposed to low-energy, high-flux D plasma at ion energies of 60 eV (a) and 200 eV (b, c) and temperatures of 365 K (a), 460 K (b), and 770 K (c) to an ion fluence of $\approx 10^{26}$ D/m². Only the surface on panel (b) was tilted by 52° to the electron beam.

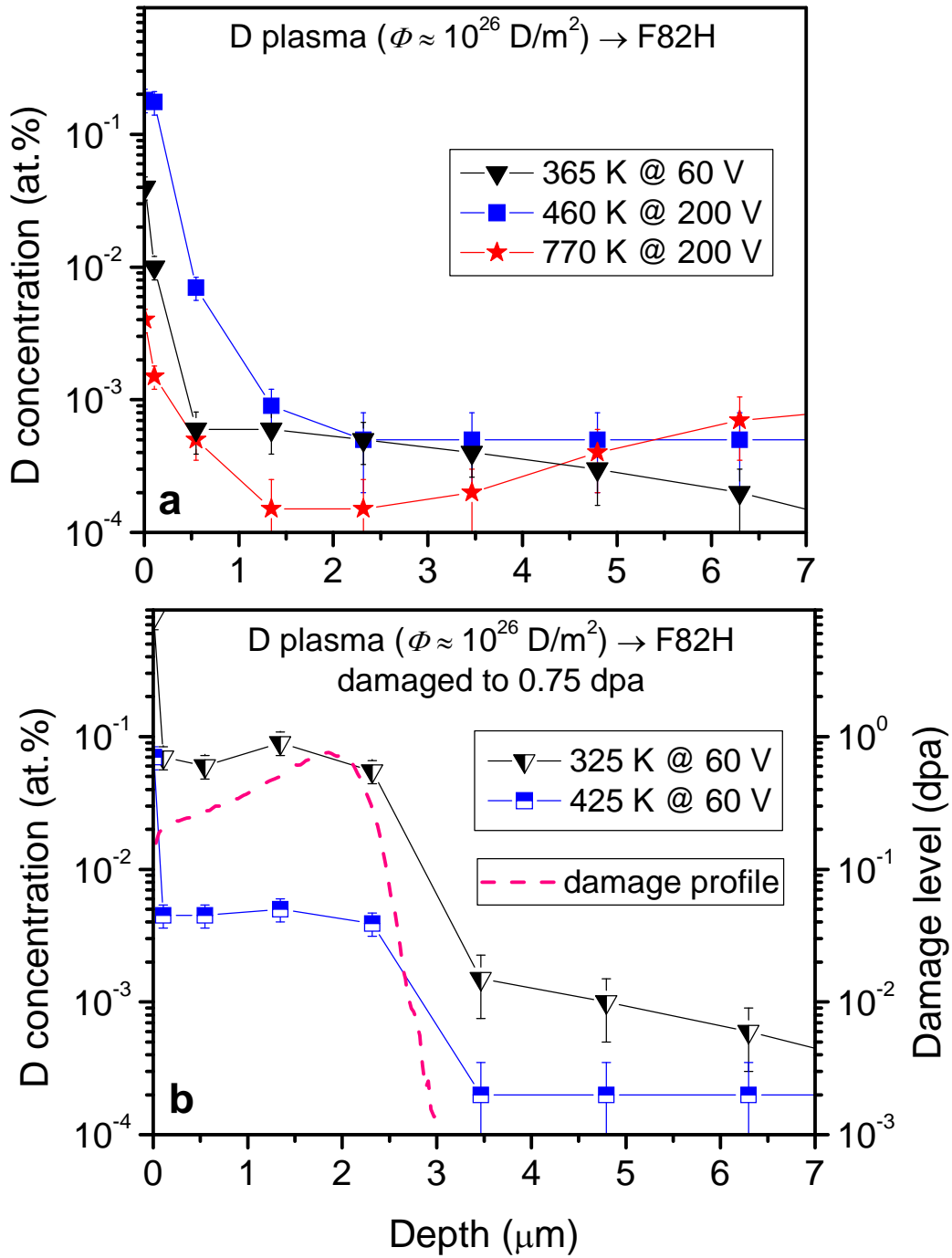


Figure 3. Depth profiles of deuterium retained in undamaged (a) and damaged (b) F82H steel after exposure to low-energy, high-flux D plasma at ion energy of 60 and 200 eV and various temperatures to an ion fluence of $\approx 10^{26}$ D/m². Deuterium ion energies and exposure temperatures are indicated in the legend. Damage depth profile, as calculated by SRIM 2008.03 [10], is also shown.

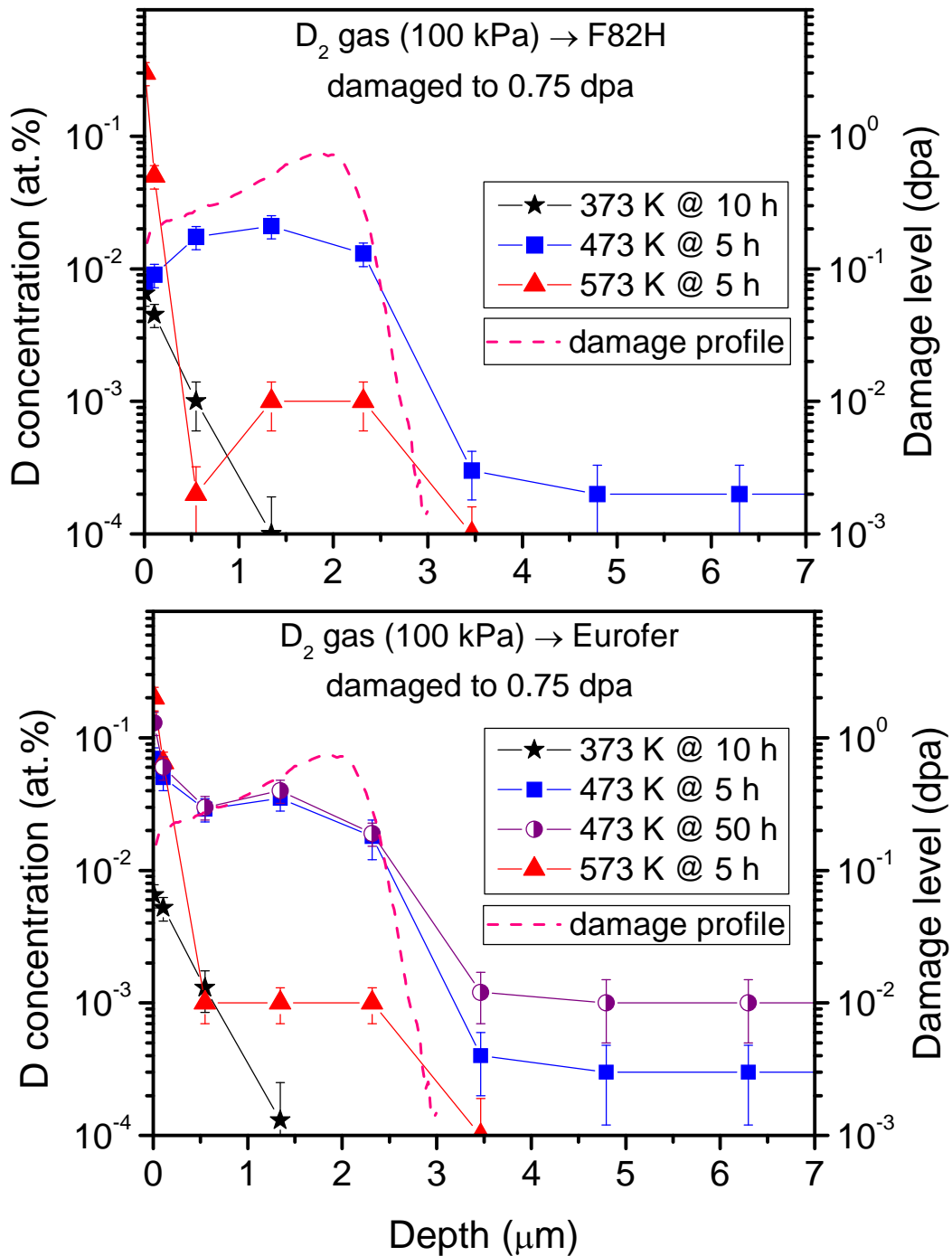


Figure 4. Depth profiles of deuterium retained in damaged F82H (a) and EUROFER97 (b) steels after exposure to D₂ gas at a pressure of 100 kPa. Exposure temperatures and exposure durations are indicated in the legends. In both panels, damage depth profile, as calculated by SRIM 2008.03 [10], is also shown.

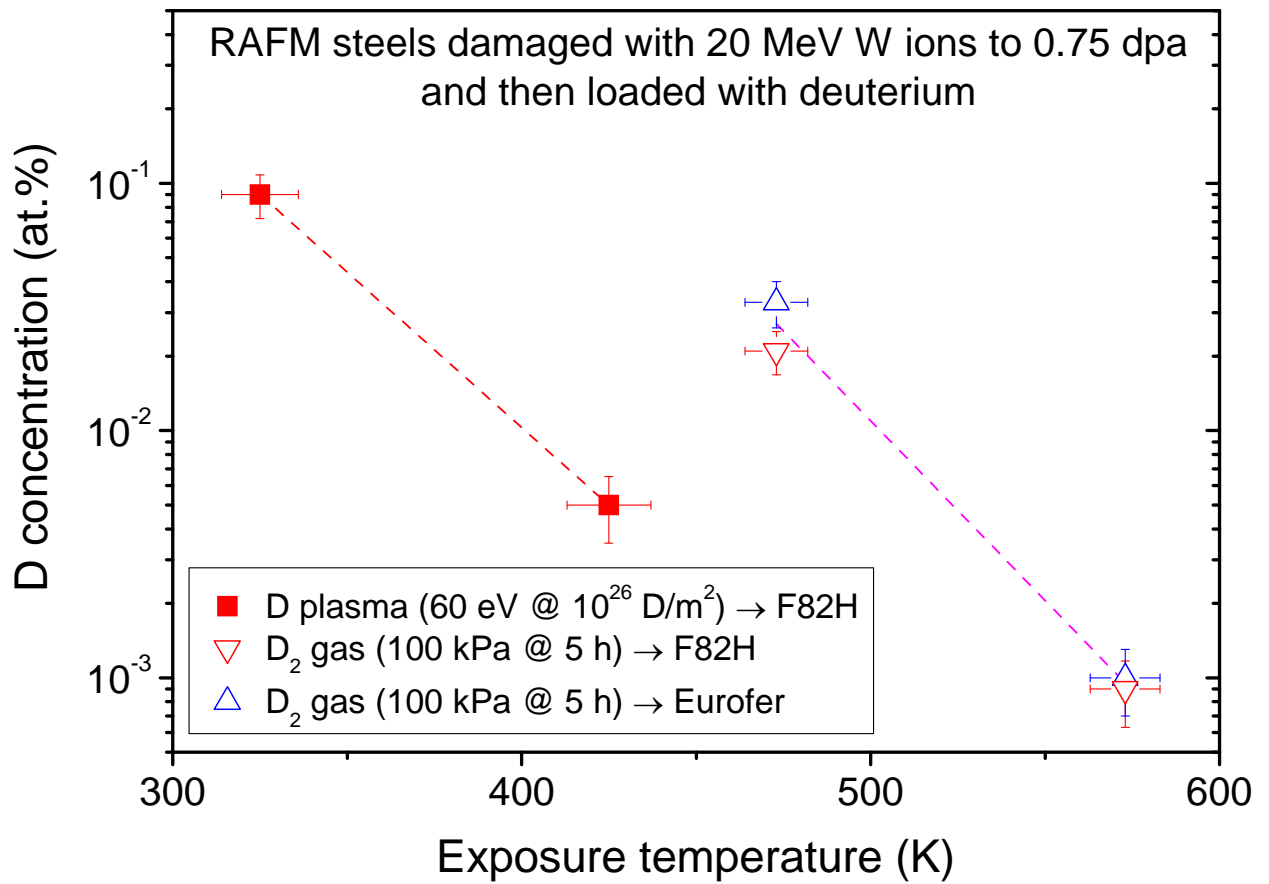


Figure 5. Concentration of deuterium retained at a depth of the damage peak in damaged F82H and EUROFER97 steels exposed to low-energy, high-flux D plasma and to D₂ gas, as a function of exposure temperature. Conditions of deuterium loading are indicated in the legend.

References

- [1] Bolt H *et al* 2004 *J. Nucl. Mater.* **329-333** 66
- [2] Mergia K and Boukos N 2008 *J. Nucl. Mater.* **373** 1
- [3] van der Schaaf B *et al* 2003 *Fusion Eng. Des.* **69** 197
- [4] Kohyama A *et al* 1996 *J. Nucl. Mater.* **233-237** 138
- [5] Tobita K *et al* 2006 *Fusion Eng. Des.* **81** 1151
- [6] Bolt H *et al* 2002 *J. Nucl. Mater.* **307-311** 43
- [7] Andersen H H and Bay H L 1981 *Sputtering by Particle Bombardment I*, ed R. Behrisch (Berlin: Springer) p 145
- [8] Alimov V Kh *et al* 2013 *J. Nucl. Mater.* <http://dx.doi.org/10.1016/j.jnucmat.2013.01.208>
- [9] Lindau R *et al* 2005 *Fusion Eng. Des.* **75-79** 989
- [10] Ziegler J F 2008 *SRIM - The Stopping and Range of Ions in Matter: ver. SRIM-2008.3* <http://srim.org>
- [11] Luo G-N *et al* 2004 *Rev. Sci. Instrum.* **75** 4374
- [12] Lindig S *et al* 2009 *Phys. Scr.* **T138** 014040
- [13] Mayer M 1997 *SIMNRA User's Guide, Rep. IPP 9/113* (Garching: Max-Planck-Institut für Plasmaphysik)
- [14] Alimov V Kh *et al* 2005 *Nucl. Instr. Meth.* **B 234** 169
- [15] Hatano Y *et al* 2013 *J. Nucl. Mater.* <http://dx.doi.org/10.1016/j.jnucmat.2013.01.018>
- [16] Serra E, Perujo A, Benamati G 1997 *J. Nucl. Mater.* **245** 108
- [17] Esteban G A *et al* 2007 *J. Nucl. Mater.* **367-370** 473